Supplementary Information (SI) for Analyst.
This journal is © The Royal Society of Chemistry 2026

Supporting Information

A single fluorescent probe for simultaneous detection of Zn^{2+}, Cd^{2+}, and Pb^{2+} in industrial wastewater with application in bio-imaging and molecular logic gates

Chandi Charan Ghosh, Snigdha Roy,[a] Sowmadeep Das,[b] Sanju Das,[c] Ambarish Ray[d] and Partha Pratim Parui*[a]

[a]*Department of Chemistry, Jadavpur University, Kolkata 700032, India*.

[b]*School of Biological Sciences, Indian Association for the Cultivation of Science, Kolkata 700032, India.*

[c]*Department of chemistry, Maulana Azad College, Kolkata 700013, India.*

[d]*Department of Chemistry, Barasat Govt. College, Kolkata 700124, India.*

Contents

Table S1: Fluorometric detection sensitivities of L_1 in different water%

DMF/water (*v*/*v*)	[a]F_x/F_0			Detection limit (μM)		
	Zn^{2+}	Cd^{2+}	Pb^{2+}	Zn^{2+}	Cd^{2+}	Pb^{2+}
9:1	8.3	15.4	2.7	0.024	0.014	0.008
4:1	8.2	15	2.5	0.025	0.015	0.008
3:2	5.4	9.2	2.1	0.08	0.050	0.025
2:3	3.9	5.1	1.9	0.120	0.081	0.041
1:4	3.6	3.1	2.8	0.150	0.101	0.060

[a]M^{2+} induced fluorescence enhancement.

Table S2: Comparison of performances of previously reported multi-metal ion sensing probes

Fluorescent probe	Metal ions detection	LOD (μM)	Response time	Applications	Ref
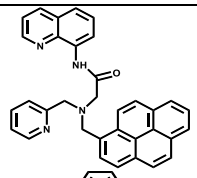	Zn^{2+}, Cd^{2+}	Zn^{2+}: 0.0185 Cd^{2+}: 0.0183	Zn^{2+}: 25 s Cd^{2+}: 30 s	(i) Food quality control, (ii) Detection in cells and mice.	1
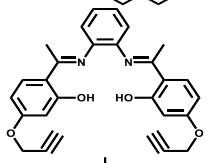	Cd^{2+}, Pb^{2+}	Cd^{2+}: 0.0129 Pb^{2+}: 0.0106	-	(i) Cell imaging	2
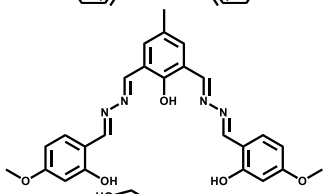	Zn^{2+}, Cd^{2+}	Zn^{2+}: 0.0027 Cd^{2+}: 0.0066	-	(i) Water, (ii) Logic gate	3
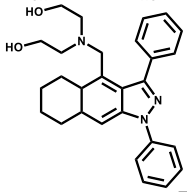	Zn^{2+}, Pb^{2+}	Zn^{2+}: 1.06 Pb^{2+}: 1.07	-	(i) River water, (ii) Logic gate	4
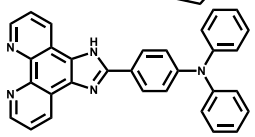	Zn^{2+}, Cd^{2+}	Zn^{2+}: 0.035 Cd^{2+}: 0.036	60 s	(i) Water, (ii) Cell imaging	5
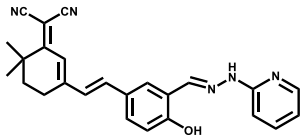	Zn^{2+}, Cd^{2+}	Zn^{2+}: 0.21 Cd^{2+}: 0.31	15 s	(i) Water, (ii) Cell imaging	6
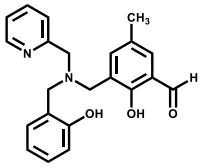	Zn^{2+}, Cd^{2+}, Pb^{2+}	Zn^{2+}: 0.025 Cd^{2+}: 0.015 Pb^{2+}: 0.008	Instant	(i) Bio-imaging, (ii) Waste water, (iii) Logic gates	This work

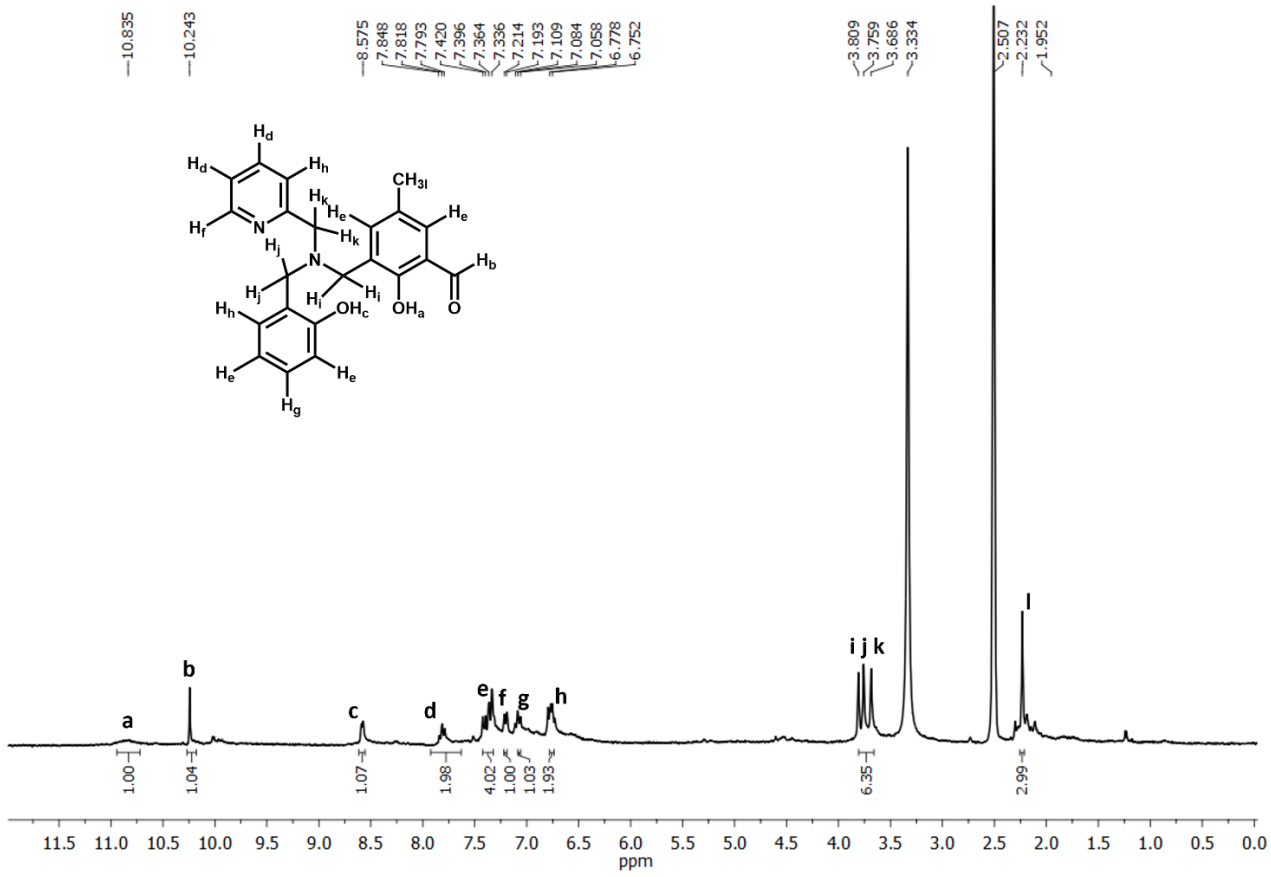

Fig. S1. ^{1}H-NMR spectrum of L_1 in DMSO-d_6.

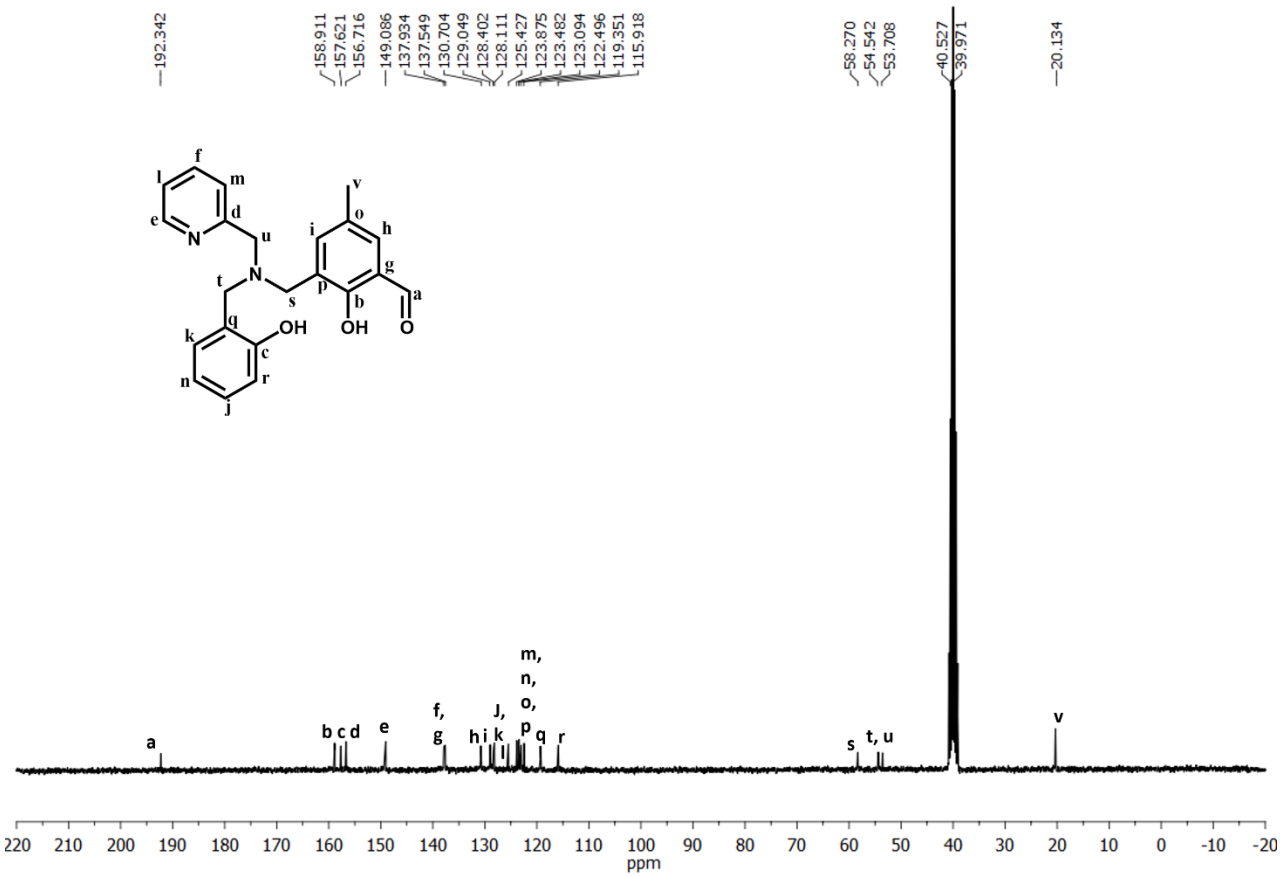

Fig. S2. ^{13}C-NMR spectrum of L_1 in DMSO-d_6.

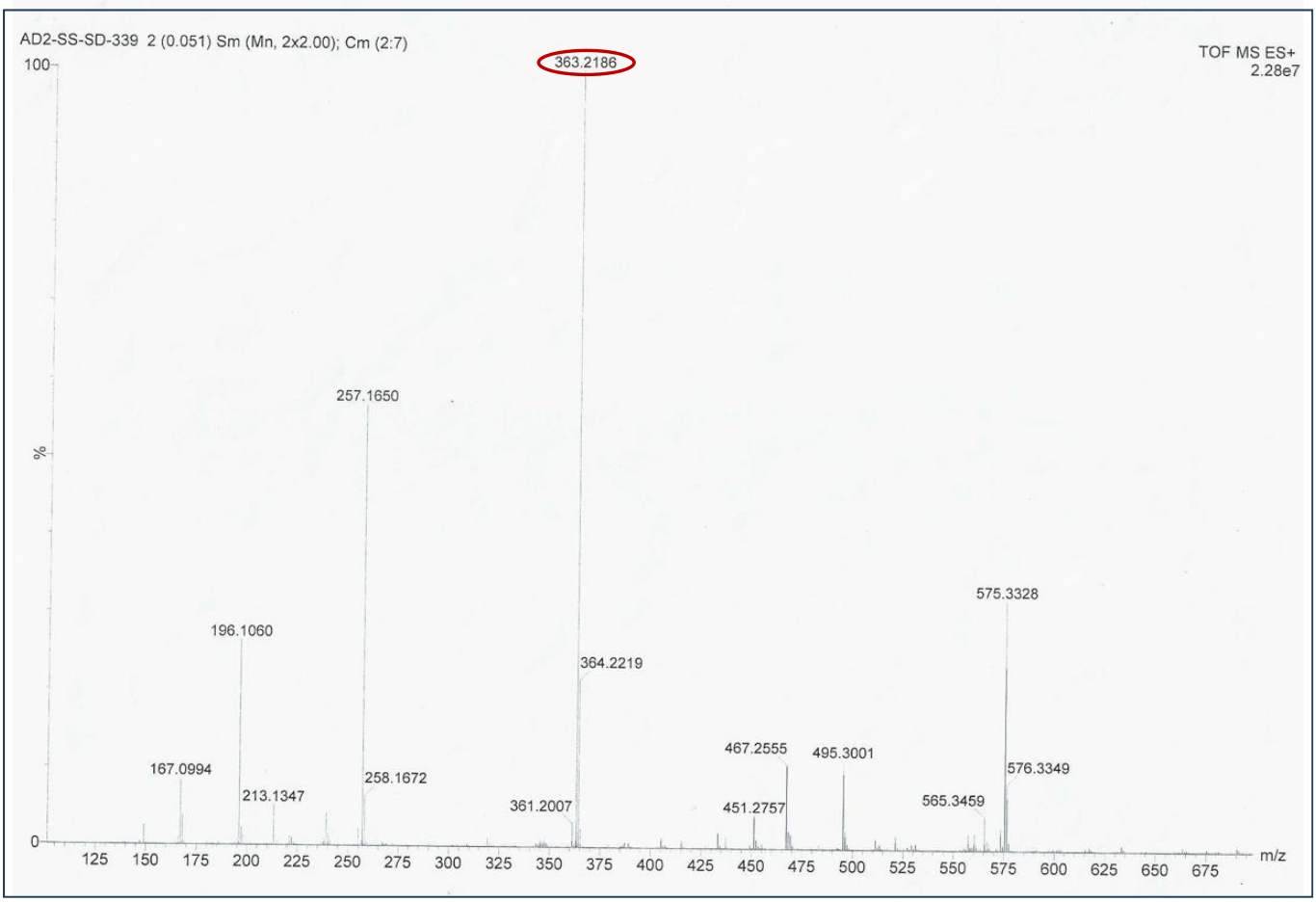

Fig. S3. ESI-MS$^+$ of L_1 (*m/z* of $[L_1+H]^+$ or $[C_{22}H_{23}N_2O_3]^+$ **363.2186** (observed) and **363.437 (**calculated).

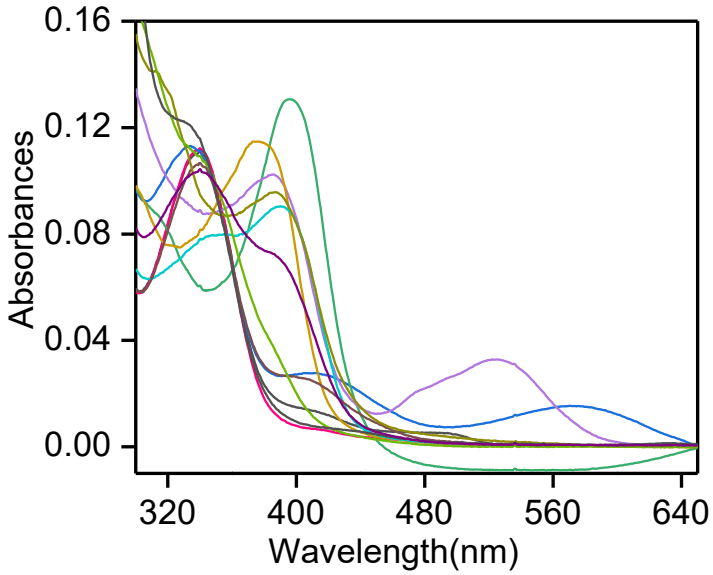

Fig. S4. UV-Vis absorption spectra of L_1 (10 μM) in the presence of different metal ions: Hg^{2+} (pink), Cr^{2+} (blue), Ni^{2+} (green), Co^{2+} (violet), Zn^{2+} (light yellow), Al^{3+} (cyan), Ba^{2+} (dark brown), Mn^{2+} (dark yellow), Pb^{2+} (olive), Sn^{2+} (gray) and Cd^{2+} (purple) (10 μM each) in DMF/water (4:1) mixed solvents at 25 °C. The spectra in the absence of metal ions is shown in black.

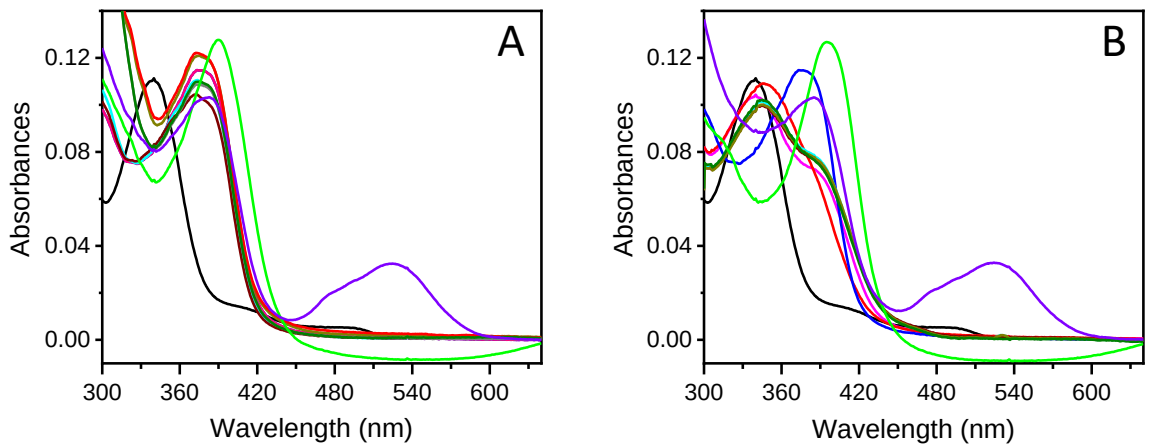

Fig. S5. Effect of various other metal ion (10 µM) on the UV-Vis absorption spectrum of (A) Zn(II)/L_1 and (B) Cd(II)/L_1 (10 µM with respect to L_1) in DMF/water (4:1) mixed solvents at 25 °C: Cr^{2+}, green; Ni^{2+}, light green; Co^{2+}, violet; Al^{3+}, cyan; Ba^{2+}, dark brown; Pb^{2+}, red; Sn^{2+}, gray; Hg^{2+}, pink; and Mn^{2+}, dark yellow) in 4:1 (v/v) DMF water mixture at 25 °C. The spectra in the absence of metal ions is shown in black.

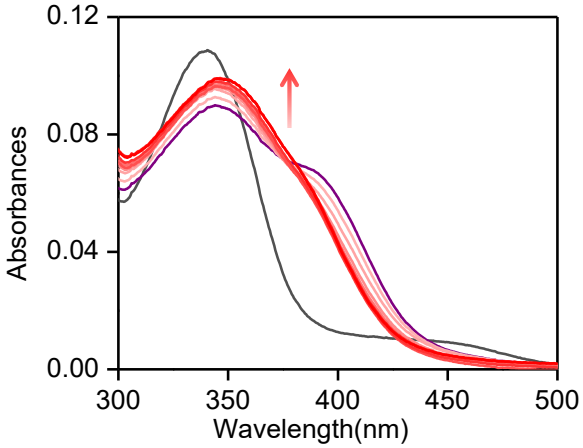

Fig. S6. Effect of increasing concentration of Pb^{2+} (0–7 μM) on the UV-Vis absorption spectrum of Cd(II)/L_1 (10 μM with respect to L_1) in DMF/water (4:1) mixed solvents at 25 °C. The intensity increase with the increase of Pb^{2+} amount are shown by arrows. The spectra of L_1 and Cd(II)/L_1 is shown in black and purple, respectively.

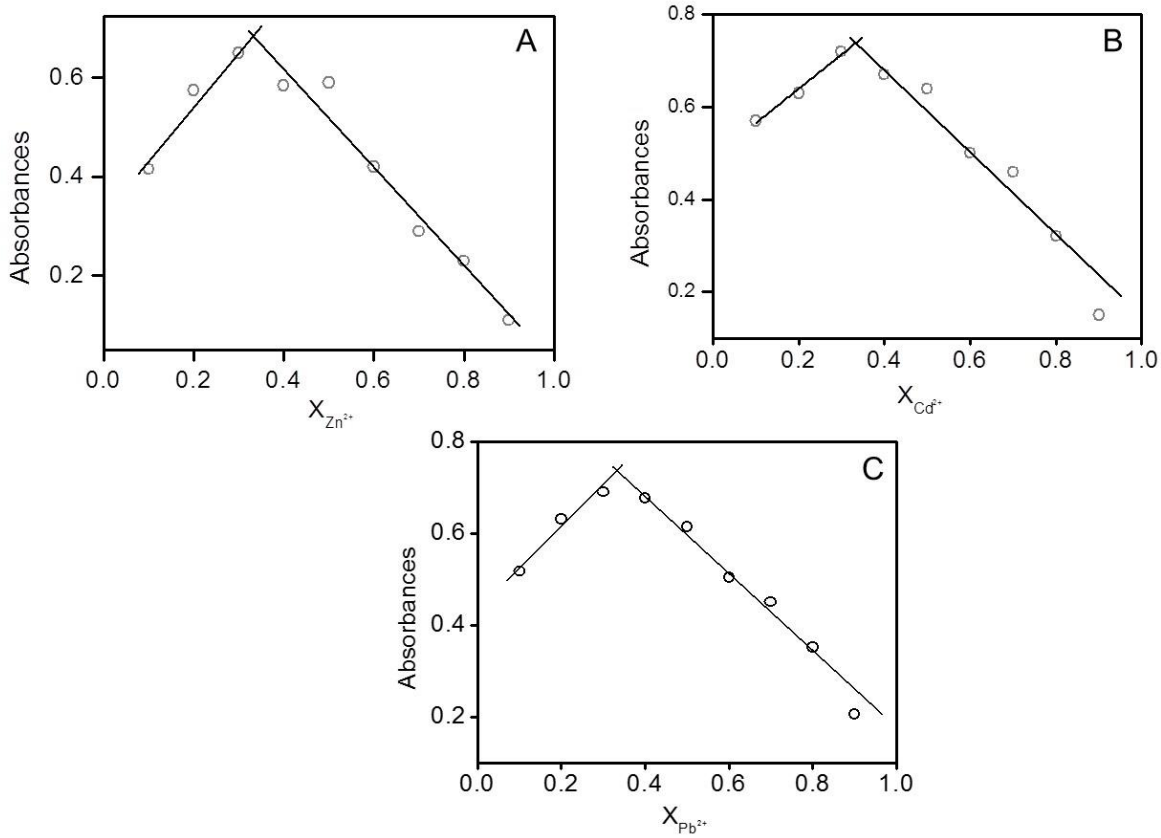

Fig. S7. Job's plot for defining binding stoichiometry of M^{2+} to L_1 for (A) Zn(II)/L_1, (B) Cd(II)/L_1 and (C) Pb(II)/L_1 in DMF/water (4:1) mixed solvents, at 25 °C.

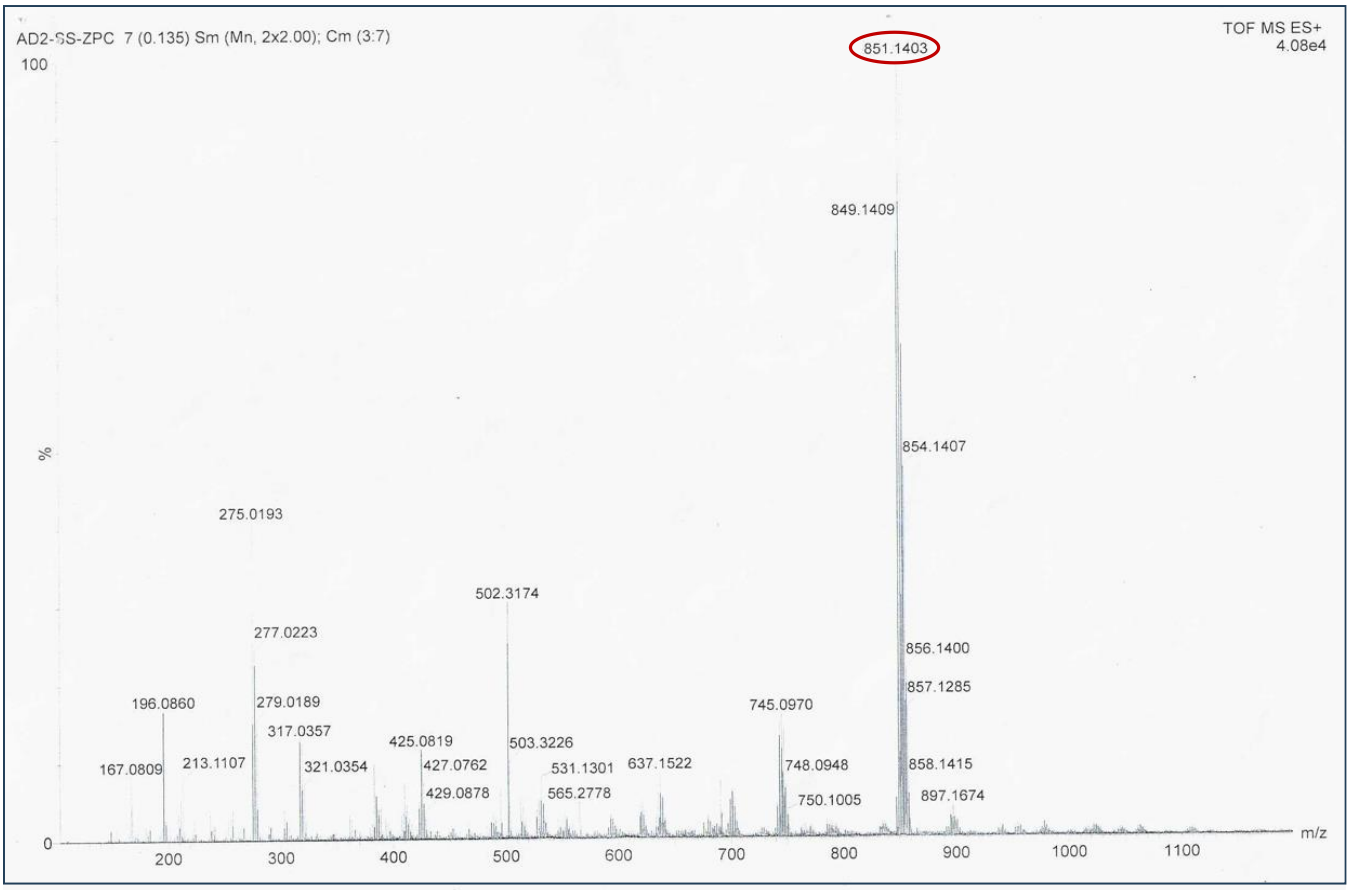

Fig. S8. ESI-MS^{+} of Zn(II)/L_1 (*m*/*z* of $[2L_1+Zn^{2+} + NO_3^-]^+$ or $[C_{44}H_{43}N_5O_9]^+$) **851.1403** (observed), **851.234 (**calculated).

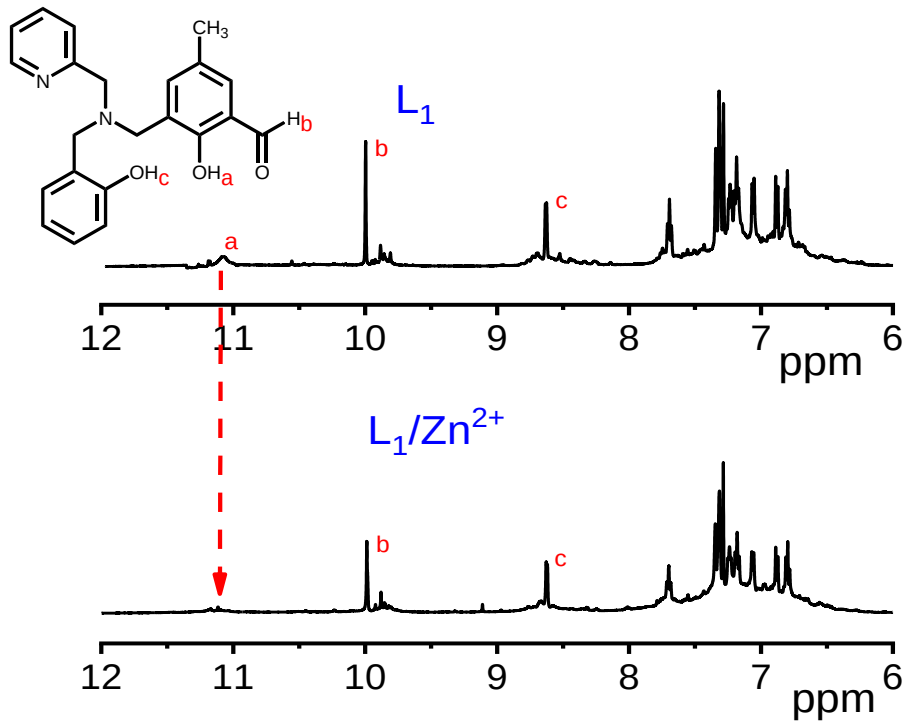

Fig. S9. ^{1}H-NMR spectra of L_1 in the absence and presence of 1.0 equiv. of anhydrous $Zn(NO_3)_2$ in DMSO-d_6.

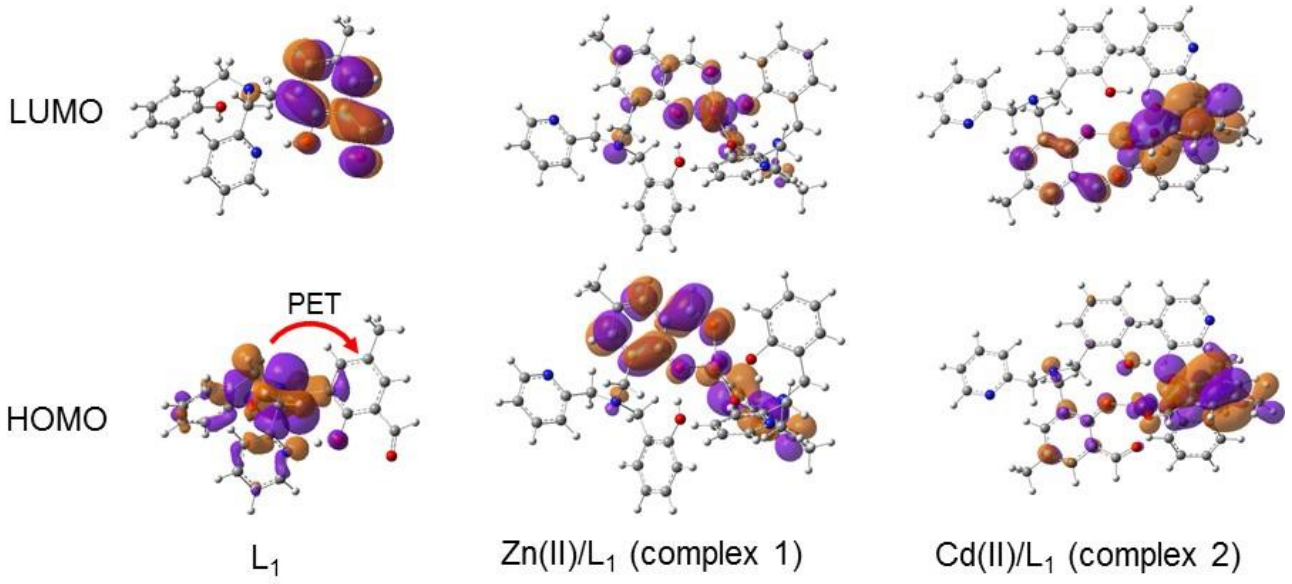

Fig. S10. Frontier molecular orbital (FMO) profiles (lower panel: HOMO and upper panel: LUMO) of L_1 and its complex with Zn(II) and Cd(II) for ground (S_0) and first excited (S_1) states are shown.

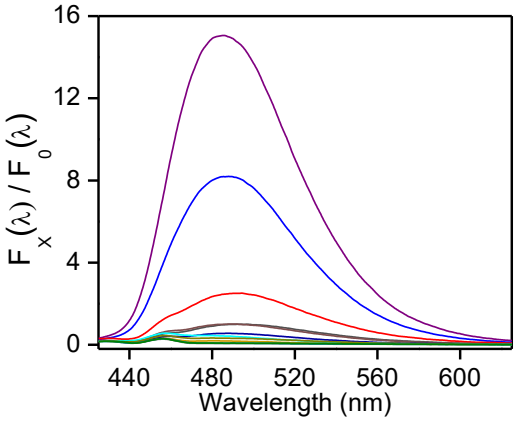

Fig. S11. Normalized fluorescence spectra ($F_x(\lambda)/F_0(\lambda)$) of L_1 (10 μM) in the presence of various metal ions: Hg^{2+} (brown), Cr^{2+}(olive), Zn^{2+} (blue), Cd^{2+} (purple), Cu^{2+} (dark cyan), Al^{3+} (cyan), Co^{2+} (violet), Mn^{2+} (dark yellow), Pb^{2+} (red), Sn^{2+} (gray) and Fe^{2+} (light yellow), K^{+} (dark blue) (10 μM each) in DMF/water (4:1) mixed solvents at 25 °C. The spectrum in the absence metal ion is shown in black. Excitation wavelength was 384 nm.

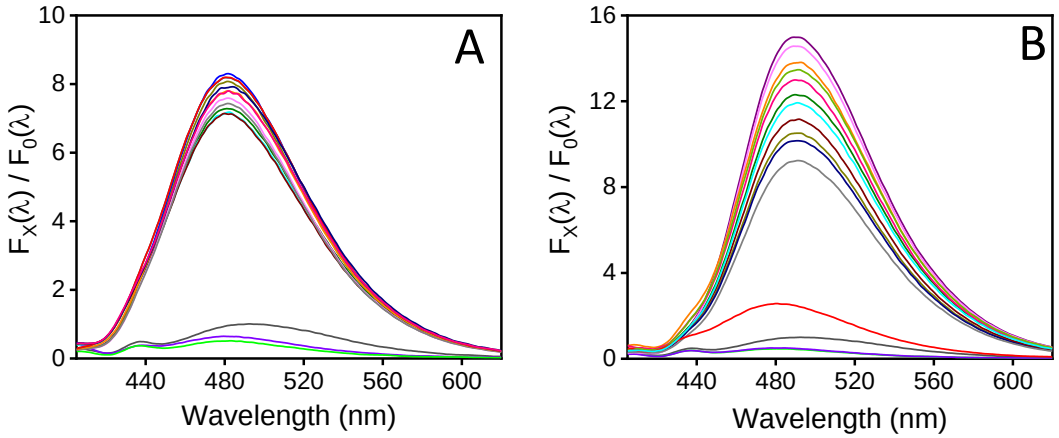

Fig. S12. Normalized fluorescence spectra ($F_x(\lambda)/F_0(\lambda)$) of (A) Zn(II)/$L_1$ and (B) Cd(II)/L_1 (10 µM with respect to L_1) in the presence and absence (A: blue and B: purple) of various metal ions (Na^+: magenta; K^+, dark blue; Mg^{2+}: olive, Ca^{2+}: orange, Cr^{2+}: dark cyan; Al^{3+}, cyan; Mn^{2+}, dark yellow; Fe^{2+}, wine; Pb^{2+}, red; Sn^{2+}, gray; Ni^{2+}, green; and Co^{2+}, violet; Hg^{2+}, pink, 100 µM each) in DMF/water (4:1) mixed solvents at 25 °C. The spectra in the absence of other metal ions are shown in (A) The spectrum in the absence metal ion is shown in black. Excitation wavelength was 384 nm.

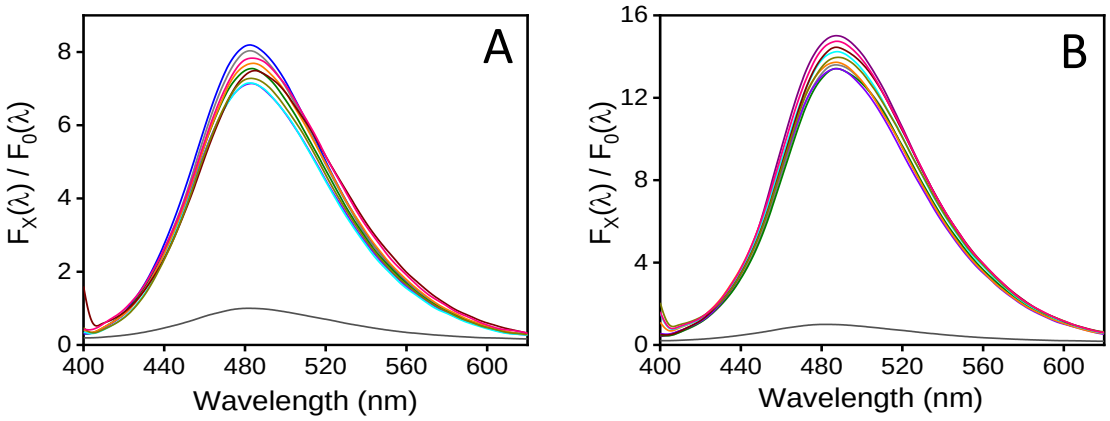

Fig. S13. Normalized fluorescence spectra ($F_x(\lambda)/F_0(\lambda)$) of (A) Zn(II)/$L_1$ and (B) Cd(II)/L_1 (10 μM with respect to L_1) in the presence and absence (A: blue and B: purple) of various common ions (Cl^-, violet; SO_4^{2-}, orange; PO_4^{2-}, cyan; HCO_3^-, wine; NO_3^-, olive; SDS, dark yellow; CTAB, grey; humic acid, pink; 1 mM each) in DMF/water (4:1) mixed solvents at 25 °C. The spectrum in the absence of ions is shown in black. Excitation wavelength was 384 nm.

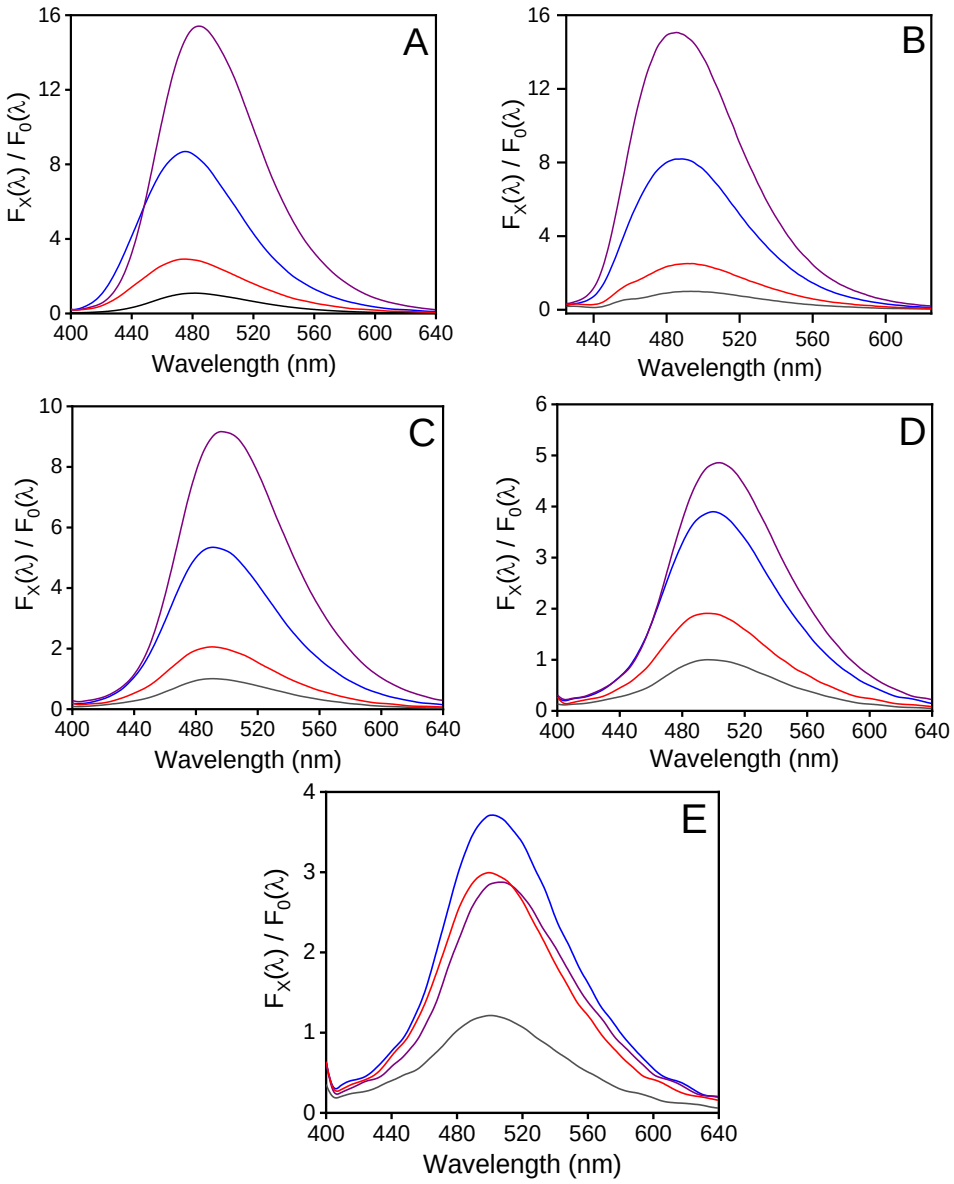

Fig. S14. Normalized fluorescence spectra ($F_x(\lambda)/F_0(\lambda)$) of M^{2+}/L_1 complex (M^{2+}: Zn^{2+} (blue), Cd^{2+} (purple) and Pb^{2+} (red)) in various mixed DMF/water medium (A: 9:1; B: 4:1; C: 3:2; D: 2:3 and E:1:4) at 25 °C. Excitation wavelength was 384 nm.

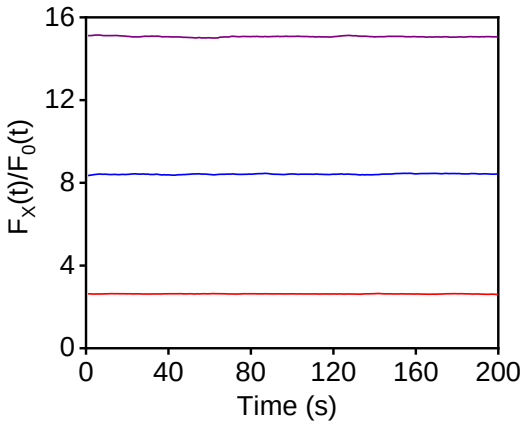

Fig. S15. Time course of normalized fluorescence intensity of L_1 ($F_x(t)/F_0(t)$) by the addition of Zn^{2+} (blue, 7 μM), Cd^{2+} (purple, 15 μM) and Pb^{2+} (red, 7 μM) in DMF/water (4:1) mixed solvents at 25 °C. Excitation wavelength was 384 nm. Emission wavelength was 484 nm.

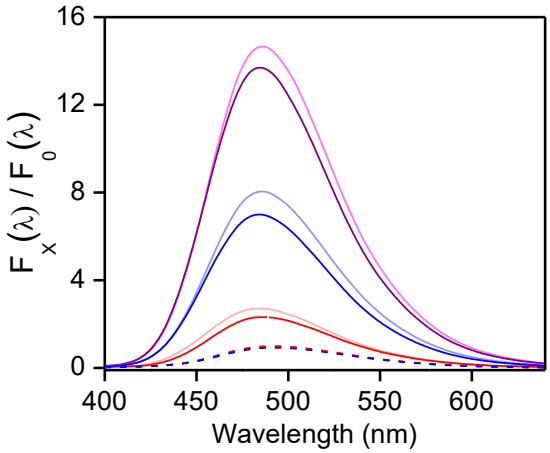

Fig. S16. Normalized fluorescence spectra ($F_x(\lambda)/F_0(\lambda)$) of M(II)/$L_1$ complex (Zn(II), blue; Cd(II), purple and Pb(II), red) in the (light color, solid) absence and (dark color, solid) presence of EDTA (10 μM) followed by (dark color, broken) addition of excess amount of corresponding metal ion in DMF/water (4:1) mixed solvents at 25 °C. Excitation wavelength was 384 nm.

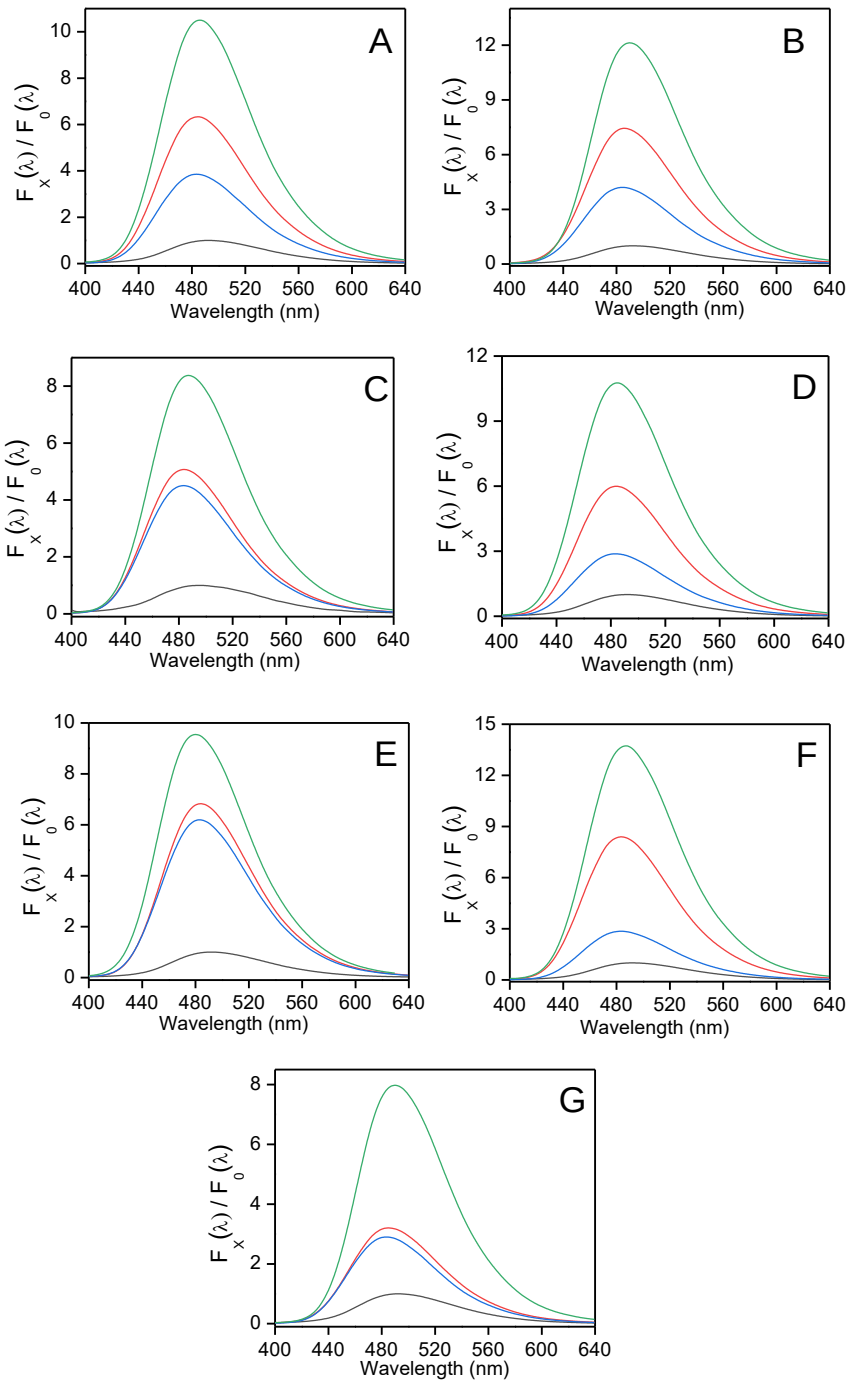

Fig. S17 Normalized fluorescence spectra ($F_x(\lambda)/F_0(\lambda)$) of M(II)/$L_1$ for various mixture of Zn^{2+}, Cd^{2+} and Pb^{2+} (total concentration, 10 μM; $[Zn^{2+}]$:$[Cd^{2+}]$:$[Pb^{2+}]$ = (A) 3.4:3.3:3.3; (B) 4.5;4.5:1.0; (C) 4.5:1.0:4.5; (D) 1.0:4.5:4.5; (E) 8.0:1.0:1.0; (F) 1.0:8.0:1.0 and (G) 1.0:1.0:8.0) in DMF/water (4:1) mixed solvents at 25 °C. The spectra obtained under various saturated L_1 concentration (A, 28 μM; B, 30 μM; C, 26 μM; D, 30 μM; E, 25 μM; F, 32 μM and G, 30 μM). The spectra is normalized by the fluorescence intensity of saturated concentration of L_1. The spectrum in the absence metal ion is shown in black. Excitation wavelength was 384 nm.

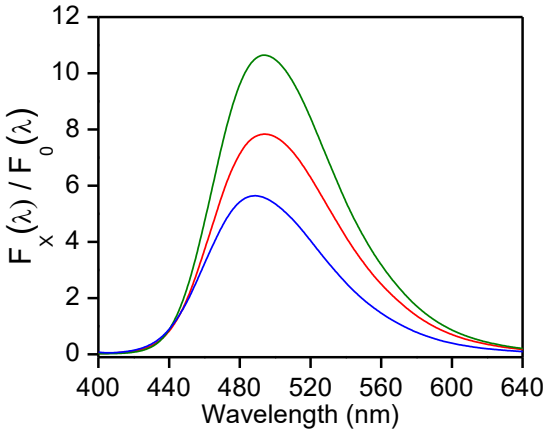

Fig. S18. Normalized fluorescence spectra ($F_x(\lambda)/F_0(\lambda)$) of M(II)/$L_1$ in DMF solvent containing 20% waste drainage water sample in the presence of saturated concentration of L_1 (red, 20 µM) followed by excess amount of Pb^{2+} (blue) or Cd^{2+} (green). The spectra is normalized by the fluorescence intensity of saturated concentration of L_1. Excitation wavelength was 384 nm.

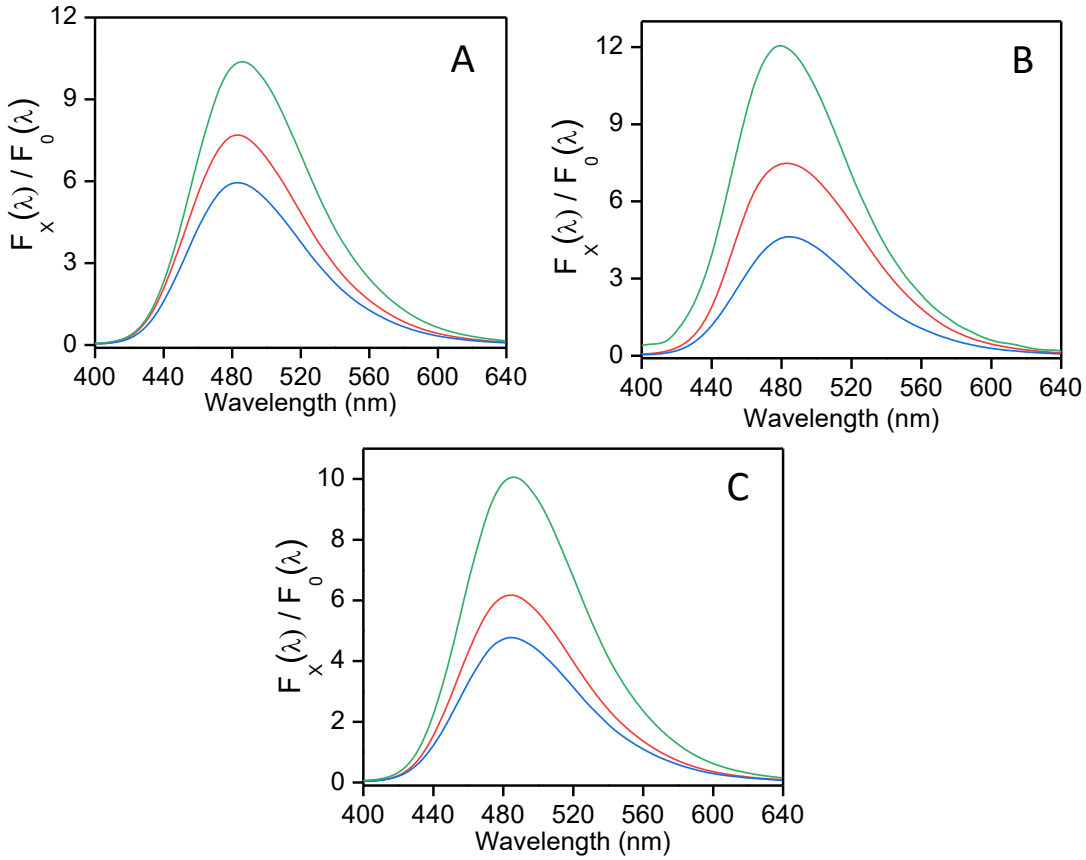

Fig. S19. Normalized fluorescence spectra ($F_x(\lambda)/F_0(\lambda)$) of M(II)/$L_1$ in DMF solvent containing 20% waste drainage water sample and (A) Zn^{2+} (2 μM), (B) Cd^{2+} (2 μM) and (C) Pb^{2+} (2 μM) in the presence of saturated concentration of L_1 (red, (A: 25 μM; B: 30 μM and C: 28 μM)) and followed by excess amount of Pb^{2+} (blue) or Cd^{2+} (green). The spectra is normalized by the fluorescence intensity of saturated concentration of L_1. Excitation wavelength was 384 nm.

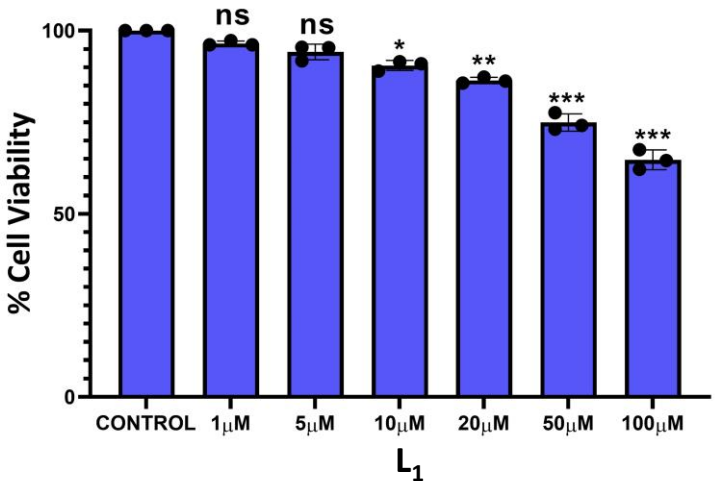

Fig. S20 MTT assay showing the percentage of viable cells after treatment with increasing concentrations of the ligand (L_1). The untreated control was used as the 100% viability reference. Bars represent mean ± SD. Statistical significance is indicated as follows: $p < 0.05$ (*), $p < 0.01$ (**), $p < 0.001$ (***), and NS = not significant.

References:

(1) H. Deng, T. Hou, X. Zhou, D. Zhang, W. Miao, C. Hou, Y. Zhang, J. Luo and X. Shen, *Analytica Chimica Acta*, 2025, **1373**, 344470.
(2) S. G. J. Andrews, S. B. J. Silviya, D. Jeyanthi, E. S. Devi, J. W. Jebaraj and C. Balakrishnan, *Analyst*, 2020, **145**, 4576–4586.
(3) R. Purkait, S. Dey and C. Sinhaa, *New J. Chem.*, 2018, **42**, 16653–16665.
(4) A. Kolbus, A. Danel, P. Moskwa, K. Szary and T. Uchacz, *Dyes and Pigments*, 2024, **223**, 111956.
(5) C. Liu, L. Ren, X. Yang, Y. Liu, H. Zhang, W. Jia and D. Zhang, *Spectrochimica Acta Part A: Molecular and Biomolecular Spectroscopy*, 2025, **328**, 125436.
(6) L. Yan, D. Lu, H. Yang and X. Wu, *Spectrochimica Acta Part A: Molecular and Biomolecular Spectroscopy*, 2023, **290**, 122243.